

A Non-Fullerene Acceptor with a Diagnostic Morphological Handle for Streamlined Screening of Donor Materials in Organic Solar Cells

Seth M. McAfee,^a Abby-Jo Payne,^a Sergey V. Dayneko,^a Gururaj P. Kini,^b Chang Eun Song,^b Jong-Cheol Lee,^b and Gregory C. Welch^{a*}

^aDepartment of Chemistry, University of Calgary, 2500 University Drive N.W., Calgary,
Alberta, T2N 1N4

^bAdvanced Materials Division, Korea Research Institute of Chemical Technology (KRICT),
141 Gajeongro, Yuseong, Daejeon 34114, Republic of Korea

*Corresponding Author
Email: gregory.welch@ucalgary.ca
Phone Number: 1 (403) 210 7603

SUPPORTING INFORMATION

TABLE OF CONTENTS

Materials and methods	S3
Synthesis	S4
Electrochemical properties	S4-5
Active layer processing	S6-7
Device fabrication	S8
Device screening	S9-11
Device optimization	S12-18
Control devices	S19-20
Device stability	S21-24
Active layer thickness	S25
Solution UV-vis spectra	S26
References	S27

Materials and methods

Materials: All compounds and solvents were purchased from Sigma-Aldrich unless indicated otherwise. Ag evaporation slugs, Mo and W evaporation boats were purchased from R.D. Mathis.

Cyclic Voltammetry (CV): All electrochemical measurements were performed using a CH Instruments potentiostat in a standard three-electrode configuration equipped with a silver wire pseudo-reference, platinum wire counter electrode and glassy carbon working electrode. The cyclic voltammetry experiments were performed in an anhydrous solution of dichloromethane (CH_2Cl_2) with ~ 0.1 M tetrabutylammoniumhexafluorophosphate (TBAPF₆) supporting electrolyte. Samples were scanned at a rate of 100 mV/s following a dry N₂ purge to deoxygenate the solution. Solution CV measurements were carried out with a sample concentration of ~ 0.5 mg/mL in CH_2Cl_2 . Estimations of the energy levels were obtained by correlating the onset ($E_{\text{ox}} \text{ Fc/Fc}^+$, $E_{\text{red}} \text{ Fc/Fc}^+$) to the normal hydrogen electrode (NHE), assuming an ionization potential of 4.80 eV for Fc/Fc⁺.¹

$$E(\text{Ionization Potential}) = - (E_{\text{ox}} + 4.80), E(\text{Electron Affinity}) = - (E_{\text{red}} + 4.80)$$

UV-Visible Spectroscopy (UV-vis): All absorption measurements were recorded using an Agilent Technologies Cary 60 UV-vis spectrometer at room temperature. All solution UV-vis experiments were run in chloroform (CHCl_3) using 2 mm quartz cuvettes and diluted 1 wt/v% solutions. Thin-films were prepared by spin-coating 1 wt/v% solutions from CHCl_3 onto Corning glass micro slides. Prior to use, glass slides were cleaned with soap and water, acetone and isopropanol, and followed by UV/ozone treatment using a Novascan UV/ozone cleaning system.

Power Conversion Efficiency (PCE) and External Quantum Efficiency (EQE): The current density-voltage (J-V) curves were measured by a Keithley 2420 source measure unit. The photocurrent was measured under AM 1.5 illumination at 100mW/cm^2 under a Solar Simulator (Newport 92251A-1000). The standard silicon solar cell (Newport 91150V) was used to calibrate light intensity. EQE was measured in a QEX7 Solar Cell Spectral Response/QE/IPCE Measurement System (PV Measurement, Model QEX7, USA) with an optical lens to focus the light into an area about 0.04cm^2 , smaller than the dot cell. The silicon photodiode was used to calibration of the EQE measurement system in the wavelength range from 300 to 1100 nm.

Atomic Force Microscopy (AFM): AFM measurements were performed by using a TT2-AFM (AFM Workshop) in tapping mode and WSxM software with an 0.01-0.025 Ohm/cm Sb (n) doped Si probe with a reflective back side aluminum coating. Samples for AFM measurement were the same ones that were used to collect the respective device parameters and EQE profiles.

Synthesis

Materials Synthesis: Small molecule acceptor **PDI-DPP-PDI** was synthesized according to our previously reported literature procedure.² **P3HT** was provided by Brilliant Matters and **PCDTBT** was provided by the research group of Mario Leclerc. **PDTT-BOBT** was provided by the research group of Jong-Cheol Lee and synthesized according to their published procedure.³

Electrochemical properties

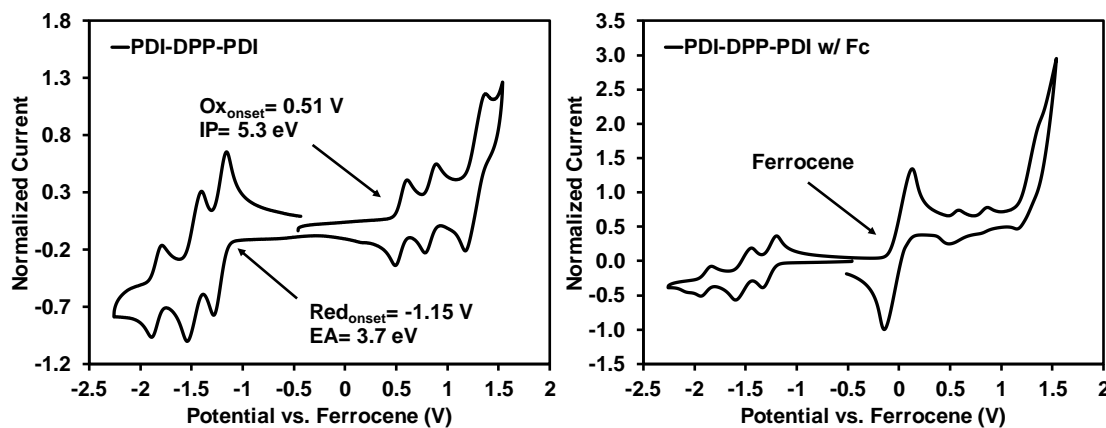


Figure S1. Cyclic voltammogram of **PDI-DPP-PDI** (left) with ferrocene reference (right).

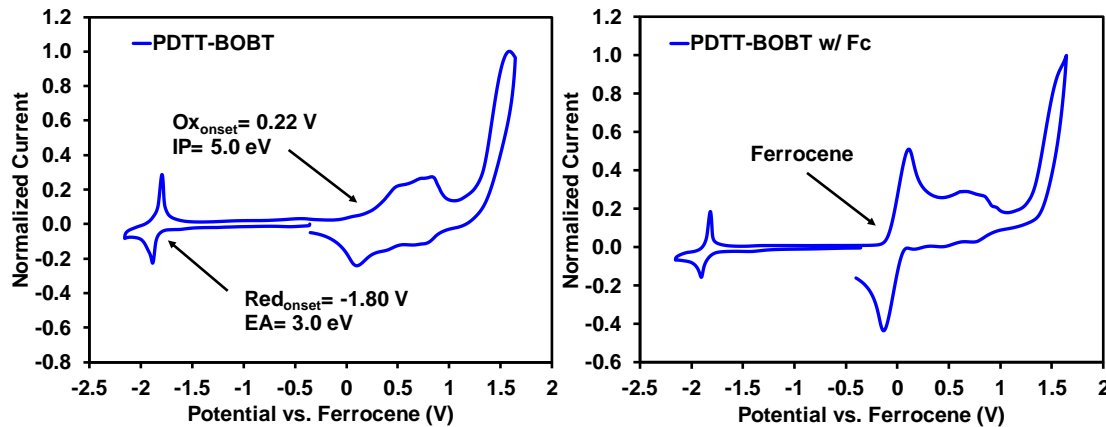


Figure S2. Cyclic voltammogram of **PDTT-BOBT** (left) with ferrocene reference (right).

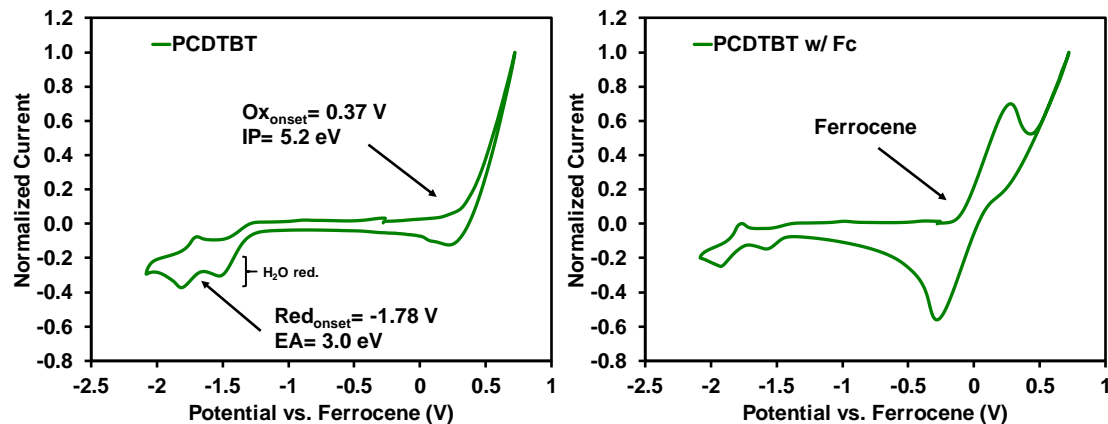


Figure S3. Cyclic voltammogram of **PCDTBT** (left) with ferrocene reference (right).

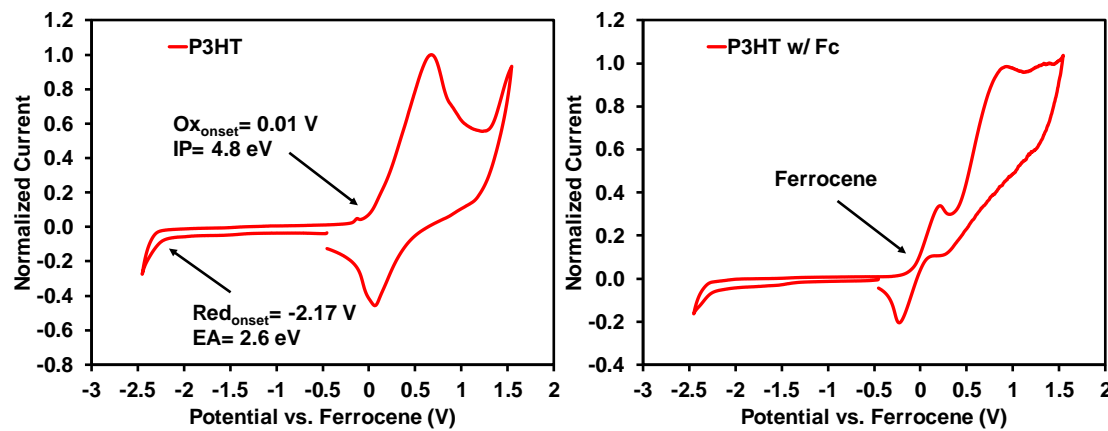


Figure S4. Cyclic voltammogram of **P3HT** (left) with ferrocene reference (right).

Active Layer Processing

To investigate the use of solvent vapour annealing as a post-deposition processing technique glass substrates were cleaned by sequentially ultra-sonicating detergent and de-ionized water, acetone and isopropanol followed by exposure to UV/ozone for 15 minutes. Thin-films of **PX:PDI-DPP-PDI** ($X = P3HT, PCDTBT, PDTT-BOBT$) in a 40:60 blend ratio were cast at 1500 rpm for 60s from a 1 wt/v% solution in chloroform.

The as-cast devices were subject to solvent vapour annealing by containing a raised as-cast substrate within a screw cap glass jar with 0.5 mL of CHCl_3 as the solvent in the bottom of the jar. Substrates were left exposed to the solvent vapour for two-minute intervals until no significant changes in the absorption profile were observed by UV-vis spectroscopy. We recognized that uninterrupted solvent vapour annealing exposure led to a more rapid change in the UV-vis profile than the two-minute interval screening and therefore the optimal solvent vapour annealing time was determined based on the time interval two minutes before the UV-vis profile did not significantly change.

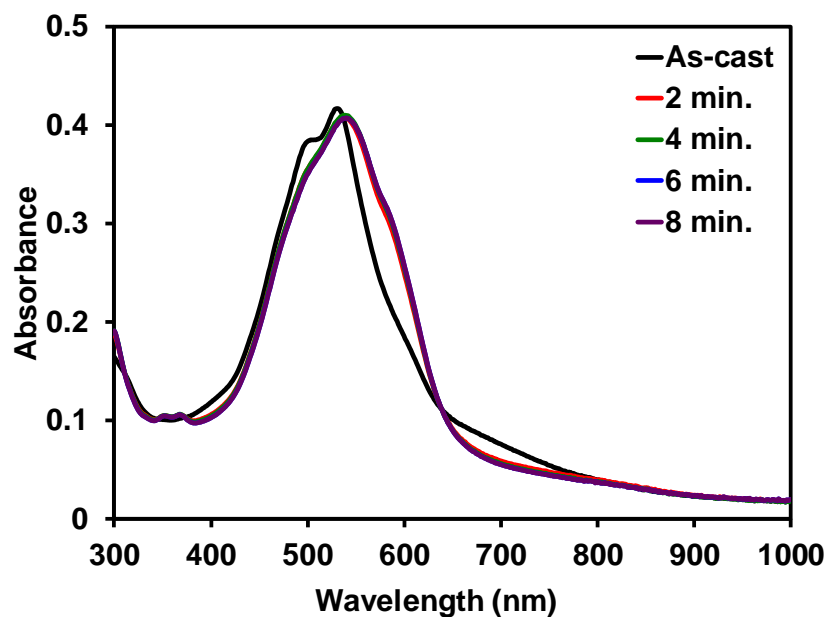


Figure S5. Optical absorption profiles for **P3HT:PDI-DPP-PDI** to screen solvent vapour annealing times. Suggested optimal time for screening: 4 minutes.

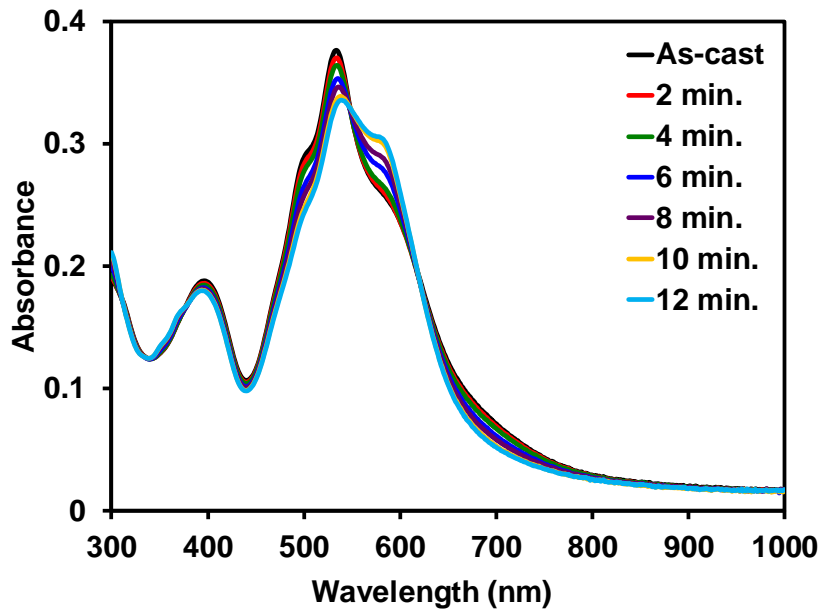


Figure S6. Optical absorption profiles for **PCDTBT:PDI-DPP-PDI** to screen solvent vapour annealing times. Suggested optimal time for screening: 8 minutes.

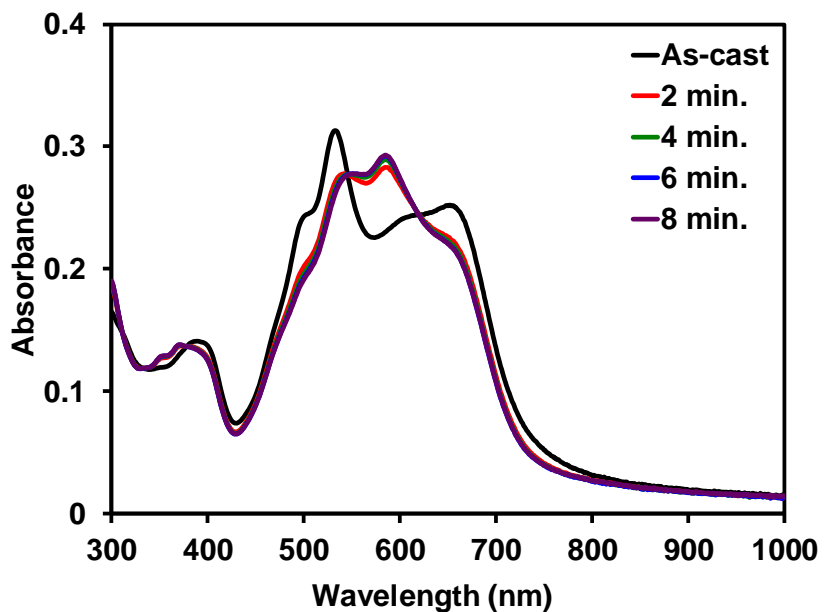


Figure S7. Optical absorption profiles for **PDTT-BOBT:PDI-DPP-PDI** to screen solvent vapour annealing times. Suggested optimal time for screening: 4 minutes.

Device Fabrication

Devices were fabricated using ITO-coated glass substrates cleaned by sequentially ultra-sonicating detergent and de-ionized water, [NaOH] and de-ionized water, acetone and isopropanol followed by exposure to UV/ozone for 30 minutes.

ZnO was deposited as a sol-gel precursor solution in air following the method of Sun *et al.*⁴ The room temperature solution was filtered and spin-cast at a speed of 4000 rpm for 60 seconds and then annealed at 200 °C in air for 15 minutes.

Active layer solutions of **P3HT** or **PCDTBT** or **PDTT-BOBT** and **PDI-DPP-PDI** or **PC₆₁BM** were prepared in air with a total concentration 10 mg/mL in chloroform unless indicated otherwise. Individual solutions were stirred overnight at room temperature. Where indicated, active layer materials were combined in varying ratios without filtration of the individual solutions and cast at room temperature in air at a speed of 1500 rpm for 60 seconds.

Post-deposition solvent vapour annealing where indicated was carried out by containing a raised as-cast substrate within a screw cap glass jar with 0.5 mL of CHCl₃ as the solvent in the bottom of the jar. Substrates were left exposed to the solvent vapour for a pre-determined time.

The substrates were then transferred to an N₂ atmosphere glovebox overnight before evaporating MoO₃ and Ag the following day. In a bell jar, 10 nm of MoO₃ followed by 100 nm of Ag were thermally deposited under vacuum (1x10⁻⁶ Torr). The active areas of resulting devices were 0.09 cm² unless indicated otherwise. Completed devices were then tested in air using a Newport 92251A-1000 AM 1.5 solar simulator which had been calibrated using a standard silicon solar cell (Newport 91150V) to obtain an irradiance level of 1000 W/m².

Device screening

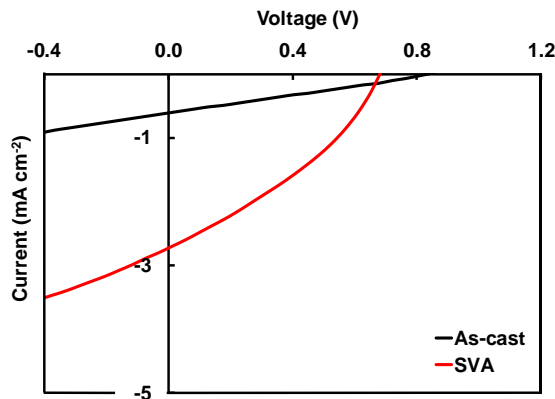


Figure S8. Current voltage curves for **P3HT:PDI-DPP-PDI** as-cast and 4 minute solvent vapour annealing with chloroform.

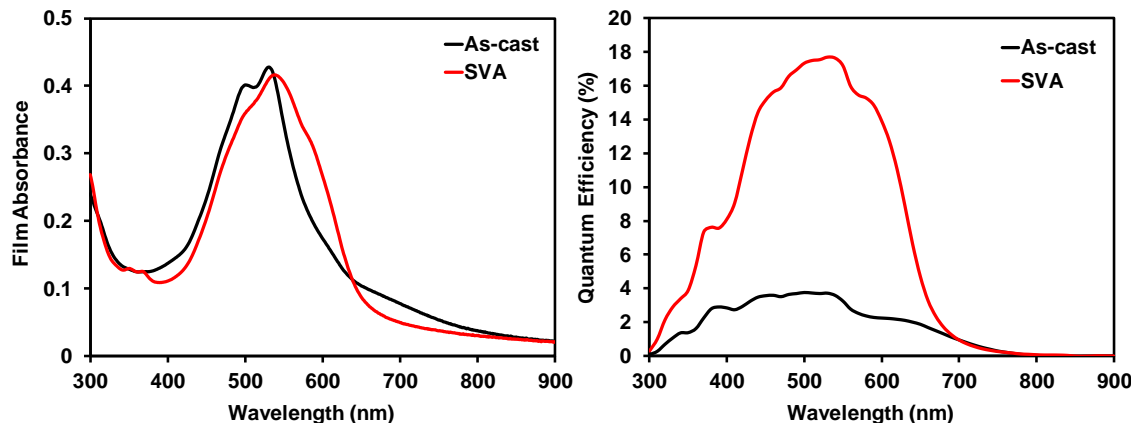


Figure S9. Optical absorption profiles (left) and EQE profiles (right) for **P3HT:PDI-DPP-PDI** as-cast and 4 minute solvent vapour annealing with chloroform.

Table S1. Device statistics for **P3HT:PDI-DPP-PDI** screening.

Processing	Voc (V)	Jsc (mAcm ⁻²)	FF (%)	PCE (%)
As-cast	0.7727	0.5873	27.1793	0.1233
As-cast	0.7919	0.5949	27.3028	0.1286
As-cast	0.8334	0.6449	26.0754	0.1401
As-cast	0.8124	0.6341	26.6082	0.1371
	0.80	0.62	26.79	0.13
Processing	Voc (V)	Jsc (mAcm ⁻²)	FF (%)	PCE (%)
SVA 4 min	0.6723	2.7210	34.8699	0.6379
SVA 4 min	0.6775	2.6396	35.1215	0.6281
SVA 4 min	0.6799	2.8907	34.3447	0.6751
SVA 4 min	0.6710	2.8758	33.7196	0.6507
	0.68	2.78	34.51	0.65

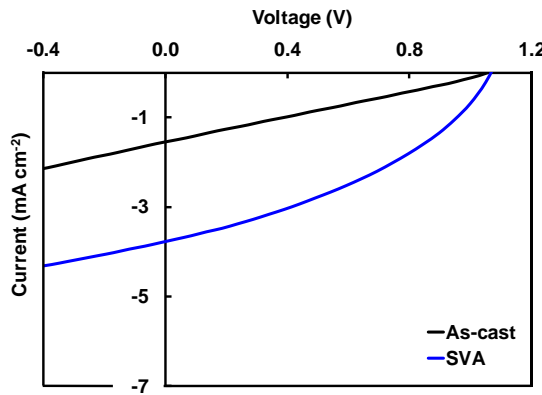


Figure S10. Current voltage curves for PCDTBT:PDI-DPP-PDI as-cast and 4 minute solvent vapour annealing with chloroform.

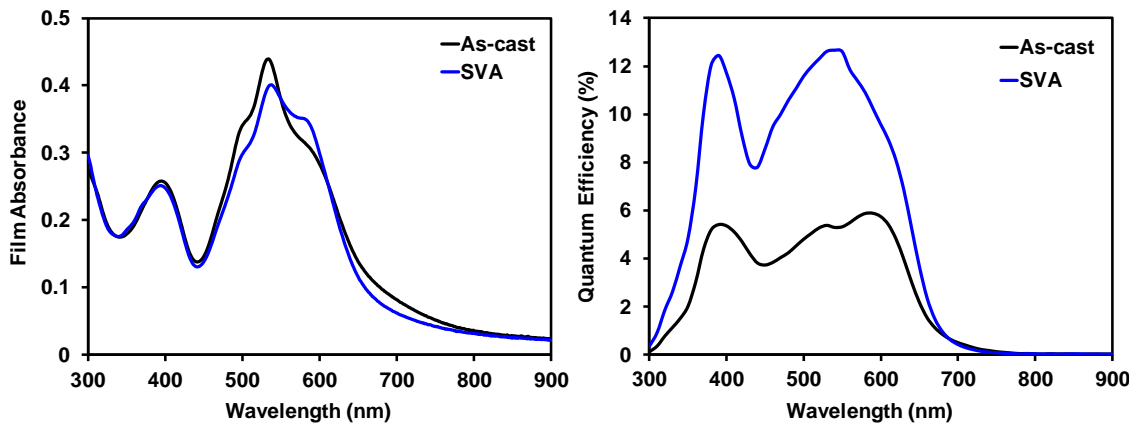


Figure S11. Optical absorption profiles (left) and EQE profiles (right) for PCDTBT:PDI-DPP-PDI as-cast and 4 minute solvent vapour annealing with chloroform.

Table S2. Device statistics for PCDTBT:PDI-DPP-PDI screening.

Processing	Voc (V)	Jsc (mAcm⁻²)	FF (%)	PCE (%)
As-cast	1.0554	1.5485	26.0631	0.4259
As-cast	1.0248	1.4116	26.5036	0.3834
As-cast	1.0218	1.4399	26.6424	0.3920
As-cast	1.0007	1.4255	27.1139	0.3868
	1.03	1.46	26.58	0.40
Processing	Voc (V)	Jsc (mAcm⁻²)	FF (%)	PCE (%)
SVA 8 min	1.0409	3.5925	37.9461	1.4189
SVA 8 min	1.0482	3.7475	37.7715	1.4837
SVA 8 min	1.0627	3.7820	37.9794	1.5264
SVA 8 min	1.0606	3.4350	37.8953	1.3806
	1.05	3.64	37.90	1.45

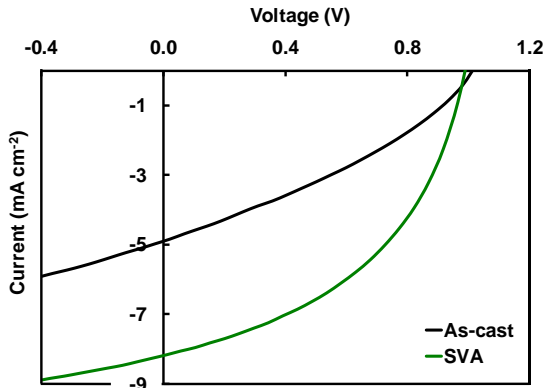


Figure S12. Current voltage curves for **PDTT-BOBT:PDI-DPP-PDI** as-cast and 4 minute solvent vapour annealing with chloroform.

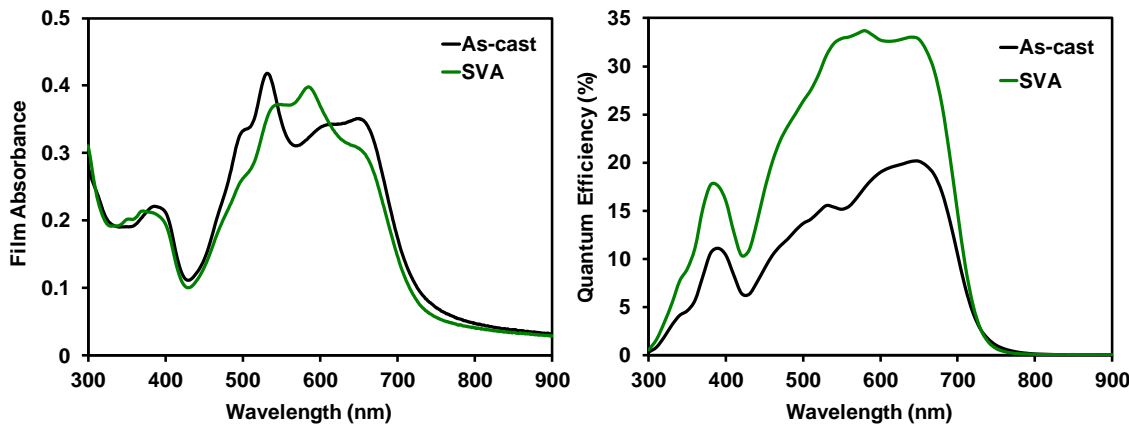


Figure S13. Optical absorption profiles (left) and EQE profiles (right) for **PDTT-BOBT:PDI-DPP-PDI** as-cast and 4 minute solvent vapour annealing with chloroform.

Table S3. Device statistics for **PDTT-BOBT:PDI-DPP-PDI** screening.

Processing	Voc (V)	Jsc (mAcm⁻²)	FF (%)	PCE (%)
As-cast	1.0221	4.7098	33.4419	1.6098
As-cast	1.0176	4.6668	33.5160	1.5916
As-cast	1.0104	4.9068	33.6090	1.6663
As-cast	0.9966	4.8728	33.5004	1.6269
	1.01	4.79	33.52	1.62
Processing	Voc (V)	Jsc (mAcm⁻²)	FF (%)	PCE (%)
SVA 4 min	0.9915	8.5893	43.3615	3.6928
SVA 4 min	0.9906	8.4719	43.5684	3.6565
SVA 4 min	0.9876	8.6899	44.1305	3.7872
SVA 4 min	0.9890	8.6898	45.4030	3.9019
	0.99	8.61	44.12	3.76

Device optimization

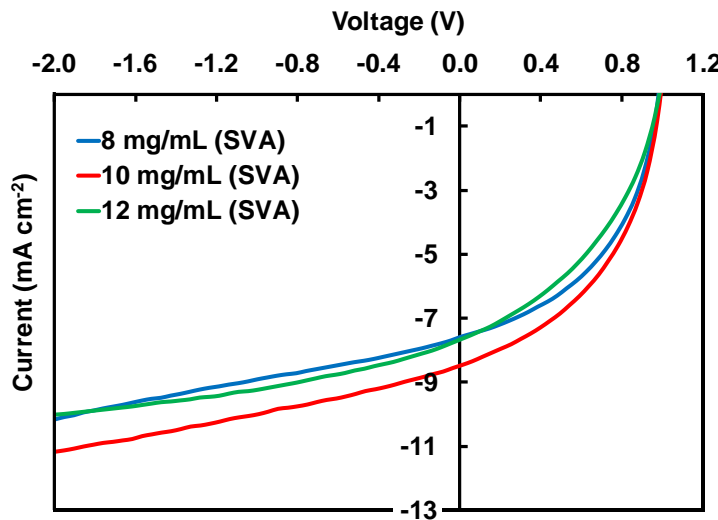


Figure S14. Current voltage curves for **PDTT-BOBT:PDI-DPP-PDI** (40:60) optimization of solution concentration upon solvent vapour annealing with chloroform for 4 minutes.

Table S4. Device statistics for **PDTT-BOBT:PDI-DPP-PDI** concentration optimization.

Concentration	Voc (V)	Jsc (mAcm-2)	FF (%)	PCE (%)	Concentration	Voc (V)	Jsc (mAcm-2)	FF (%)	PCE (%)
8 mg/mL	0.9801	7.5017	46.2742	3.4023	12 mg/mL	0.9865	7.7586	40.8159	3.1241
8 mg/mL	0.9690	7.3815	45.4192	3.2488	12 mg/mL	0.9522	7.6556	39.9287	2.9107
8 mg/mL	0.9821	7.5895	47.1971	3.5180	12 mg/mL	0.9821	7.7172	40.3952	3.0614
	0.98	7.49	46.30	3.39		0.97	7.71	40.38	3.03
Concentration	Voc (V)	Jsc (mAcm-2)	FF (%)	PCE (%)	Concentration	Voc (V)	Jsc (mAcm-2)	FF (%)	PCE (%)
10 mg/mL	0.9952	8.4509	45.7790	3.8502	10 mg/mL	0.9836	8.4508	45.2625	3.7623
10 mg/mL	0.9899	8.4823	45.9202	3.8556	10 mg/mL	0.99	8.46	45.65	3.82

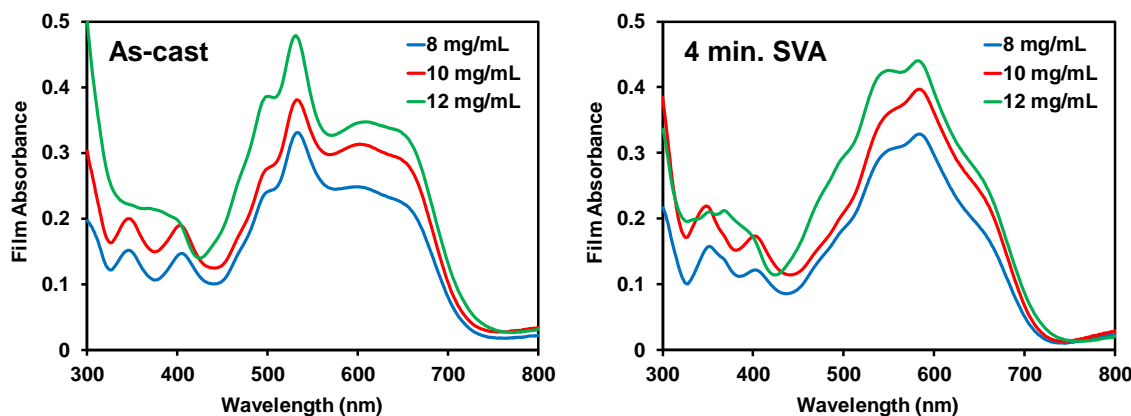


Figure S15. Optical absorption profiles for varying concentrations as-cast (left) and 4 minute solvent vapour annealed (right).

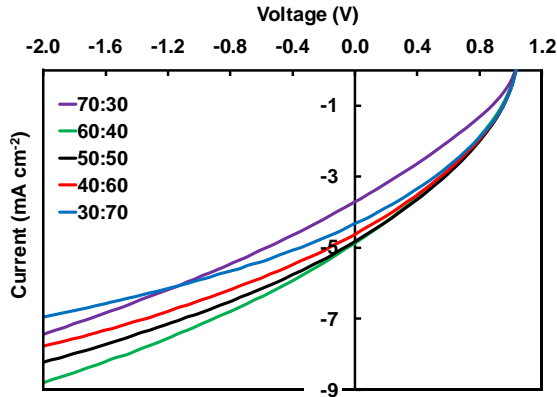


Figure S16. Current voltage curves for **PTTT-BOBT:PDI-DPP-PDI** optimization of as-cast active layer ratios.

Table S5. Device statistics for **PTTT-BOBT:PDI-DPP-PDI** as-cast ratio optimization.

Ratio	Voc (V)	Jsc (mAcm-2)	FF (%)	PCE (%)	Ratio	Voc (V)	Jsc (mAcm-2)	FF (%)	PCE (%)
70/30	1.0244	3.6076	31.5741	1.1551	40/60	1.0305	4.7000	35.0188	1.6960
70/30	1.0201	3.8118	31.8498	1.2385	40/60	1.0151	4.4829	35.6468	1.6222
70/30	1.0232	3.5785	31.1479	1.1405	40/60	1.0221	4.7098	33.4419	1.6098
70/30	1.0244	3.7214	31.4924	1.2005	40/60	1.0187	4.6322	33.9017	1.5998
	1.02	3.68	31.52	1.18		1.02	4.63	34.50	1.63
Ratio	Voc (V)	Jsc (mAcm-2)	FF (%)	PCE (%)	Ratio	Voc (V)	Jsc (mAcm-2)	FF (%)	PCE (%)
60/40	1.0278	4.8933	33.3916	1.6794	30/70	1.0311	4.2688	35.9391	1.5819
60/40	1.0243	4.7568	33.3339	1.6242	30/70	1.0306	4.1595	36.2019	1.5519
60/40	1.0256	4.8392	33.5451	1.6648	30/70	1.0326	4.3627	36.4557	1.6422
60/40	1.0198	4.5595	33.8925	1.5759	30/70	1.0112	4.1638	37.4729	1.5777
	1.02	4.76	33.54	1.64		1.03	4.24	36.52	1.59
Ratio	Voc (V)	Jsc (mAcm-2)	FF (%)	PCE (%)					
50/50	1.0270	4.9362	34.3336	1.7405					
50/50	1.0219	4.7923	34.3805	1.6837					
50/50	1.0275	4.8840	34.9540	1.7540					
50/50	1.0248	4.7106	34.9016	1.6848					
	1.03	4.83	34.64	1.72					

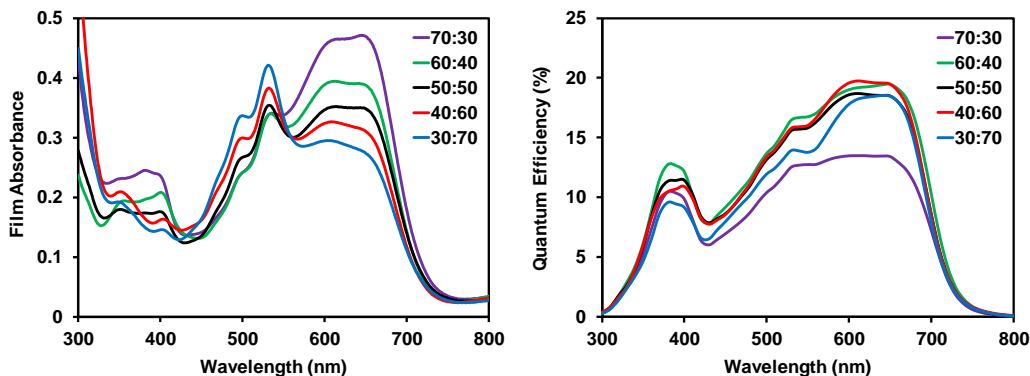


Figure S17. Optical absorption profiles (left) and external quantum efficiencies (right) for varying as-cast ratios.

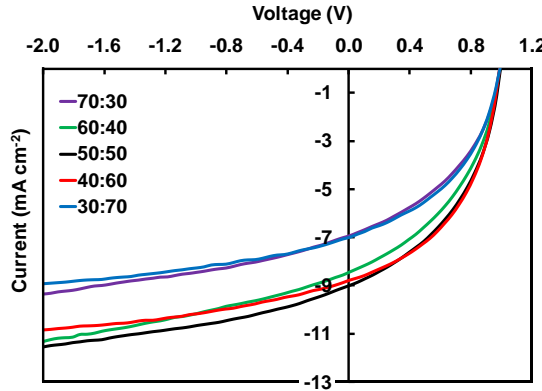


Figure S18. Current voltage curves for PTTT-BOBT:PDI-DPP-PDI optimization of 4 minute solvent vapour annealed active layer ratios.

Table S6. Device statistics for PTTT-BOBT:PDI-DPP-PDI 4 minute solvent vapour annealed ratio optimization.

Ratio	Voc (V)	Jsc (mAcm-2)	FF (%)	PCE (%)	Ratio	Voc (V)	Jsc (mAcm-2)	FF (%)	PCE (%)
70/30	0.9831	6.8362	43.0254	2.8916	40/60	0.992249	8.3189	43.9551	3.6283
70/30	0.9751	5.8149	43.7340	2.4797	40/60	0.9906	8.4719	43.5684	3.6565
70/30	0.9877	6.9471	42.9979	2.9504	40/60	0.9873	8.6023	47.1190	4.0018
70/30	0.9806	5.9836	43.4312	2.5483	40/60	0.9899	8.8904	46.8115	4.1197
	0.98	6.40	43.30	2.72		0.99	8.57	45.36	3.85
60/40	0.9866	8.3674	42.7371	3.5280	30/70	0.9612	7.7724	39.8200	2.9750
60/40	0.9794	7.2419	43.2978	3.0709	30/70	0.9891	6.9340	44.4235	3.0468
60/40	0.9883	8.4849	43.0123	3.6069	30/70	0.9717	8.0678	40.4534	3.1712
60/40	0.9898	7.2448	44.3770	3.1823	30/70	0.9909	7.1270	43.7342	3.0886
	0.99	7.83	43.36	3.35		0.98	7.48	42.11	3.07
50/50	0.9893	8.9182	43.9447	3.8770					
50/50	0.9885	7.9472	45.2703	3.5565					
50/50	0.9924	9.0329	44.5496	3.9935					
50/50	0.9857	7.9501	45.1580	3.5389					
	0.99	8.46	44.73	3.74					

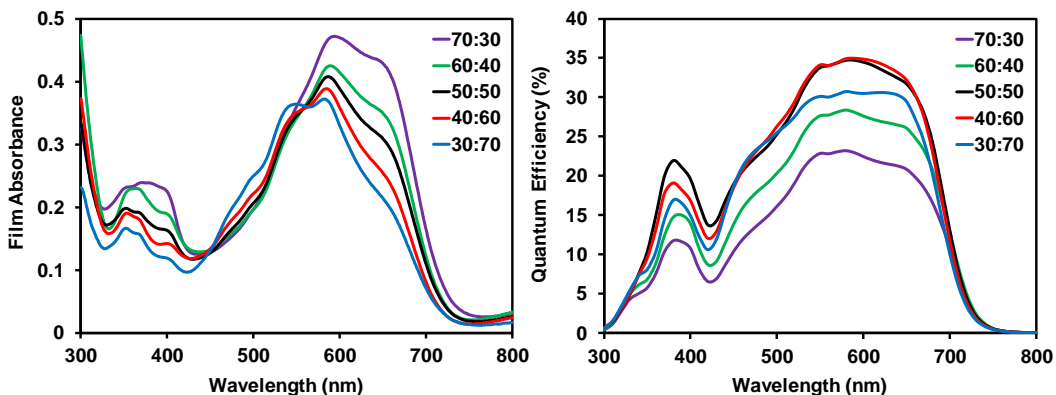


Figure S19. Optical absorption profiles (left) and external quantum efficiencies (right) for 4 minute solvent vapour annealed ratios.

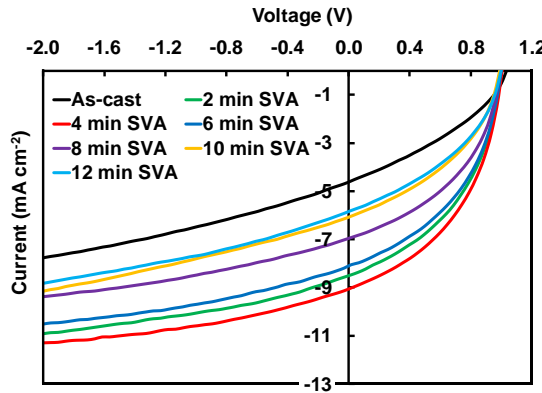


Figure S20. Current voltage curves for **PDTT-BOBT:PDI-DPP-PDI** optimization of solvent vapour annealing time.

Table S7. Device statistics for **PDTT-BOBT:PDI-DPP-PDI** solvent vapour annealing time optimization.

SVA time	Voc (V)	Jsc (mAcm-2)	FF (%)	PCE (%)	SVA time	Voc (V)	Jsc (mAcm-2)	FF (%)	PCE (%)
As-cast	1.0305	4.7000	35.0188	1.6960	8 min	0.980054	6.2043	43.9815	2.6743
As-cast	1.0151	4.4829	35.6468	1.6222	8 min	0.9810	7.0040	43.0570	2.9585
As-cast	1.0221	4.7098	33.4419	1.6098	8 min	0.9913	6.9986	44.3997	3.0805
As-cast	1.0187	4.6322	33.9017	1.5998	8 min	0.9759	6.1310	43.4825	2.6017
	1.02	4.63	34.50	1.63		0.98	6.58	43.73	2.83
SVA time	Voc (V)	Jsc (mAcm-2)	FF (%)	PCE (%)	SVA time	Voc (V)	Jsc (mAcm-2)	FF (%)	PCE (%)
2 min	0.9914	8.4383	45.0551	3.7693	10 min	0.9812	5.3126	40.9750	2.1360
2 min	0.9996	8.5338	45.1022	3.8474	10 min	0.9868	6.0473	41.3064	2.4650
2 min	0.9881	8.5832	42.5332	3.6073	10 min	0.9954	5.5738	43.2779	2.4010
2 min	0.9912	8.4812	44.0632	3.7044	10 min	0.9880	6.1082	41.1083	2.4808
	0.99	8.51	44.19	3.73		0.99	5.76	41.67	2.37
SVA time	Voc (V)	Jsc (mAcm-2)	FF (%)	PCE (%)	SVA time	Voc (V)	Jsc (mAcm-2)	FF (%)	PCE (%)
4 min	0.9946	9.1318	43.7196	3.9707	12 min	0.9983	5.8707	40.4327	2.3696
4 min	0.9975	8.9313	45.7378	4.0748	12 min	0.9900	5.4648	40.7199	2.2031
4 min	0.9916	9.1309	43.6771	3.9547	12 min	0.9944	5.8665	39.7573	2.3192
4 min	1.0028	9.0826	45.5793	4.1515	12 min	0.9847	5.2994	40.2751	2.1017
	1.00	9.07	44.68	4.04		0.99	5.63	40.30	2.25
SVA time	Voc (V)	Jsc (mAcm-2)	FF (%)	PCE (%)					
6 min	0.9800	7.5873	43.7829	3.2555					
6 min	0.9929	8.0028	45.1120	3.5845					
6 min	0.9823	7.7177	43.4511	3.2941					
6 min	0.9986	8.1026	44.9001	3.6330					
	0.99	7.85	44.31	3.44					

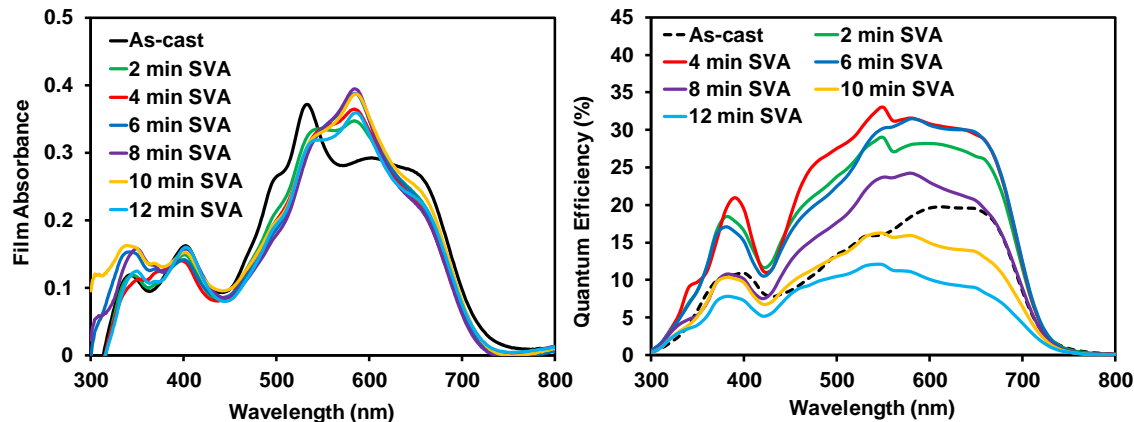


Figure S21. Optical absorption profiles (left) external quantum efficiencies (right) for solvent vapour annealing time.

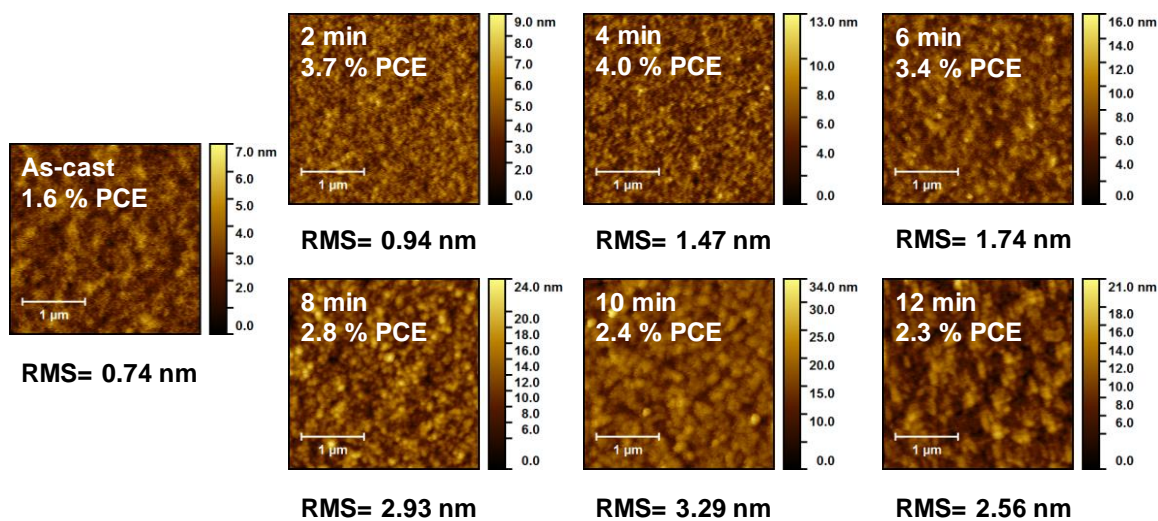


Figure S22. AFM images for solvent vapour annealing time optimization.

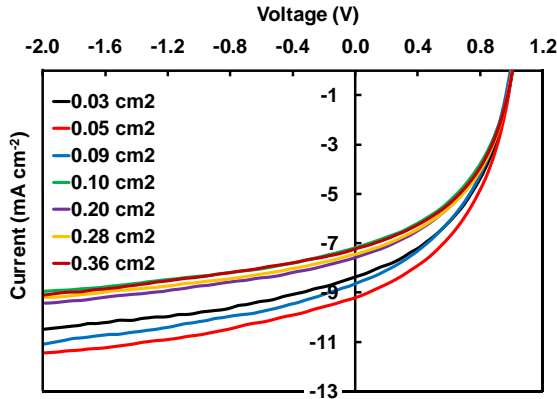


Figure S23. Current voltage curves for **PDTT-BOBT:PDI-DPP-PDI** optimization of device size.

Table S8. Device statistics for **PDTT-BOBT:PDI-DPP-PDI** device size optimization.

Device Size	Voc (V)	Jsc (mAcm-2)	FF (%)	PCE (%)	Device Size	Voc (V)	Jsc (mAcm-2)	FF (%)	PCE (%)
0.03 cm²	1.0066	8.4351	44.6788	3.7938	0.10 cm²	1.0025	7.2040	45.2296	3.2665
0.03 cm²	1.0010	7.7522	45.1306	3.5022	0.10 cm²	0.9980	7.2769	44.8873	3.2597
0.03 cm²	0.9997	7.9933	44.8326	3.5826		1.00	7.24	45.06	3.26
0.03 cm²	1.0076	8.3503	44.9422	3.7813					
	1.00	8.13	44.90	3.66	Device Size	Voc (V)	Jsc (mAcm-2)	FF (%)	PCE (%)
					0.20 cm²	1.0016	7.5947	45.0781	3.4291
Device Size	Voc (V)	Jsc (mAcm-2)	FF (%)	PCE (%)	0.20 cm²	1.0000	7.3386	45.1426	3.3128
0.05 cm²	0.9997	8.2852	44.9271	3.7212		1.00	7.47	45.11	3.37
0.05 cm²	1.0014	9.0421	44.3718	4.0179	Device Size	Voc (V)	Jsc (mAcm-2)	FF (%)	PCE (%)
0.05 cm²	1.0032	9.2411	44.8447	4.1575	0.20 cm²	1.0053	7.4500	46.1658	3.4575
0.05 cm²	1.0026	8.6569	44.6916	3.8789	0.28 cm²	0.9973	7.6634	43.9780	3.3610
0.05 cm²	0.9948	8.7498	43.2284	3.7627	0.28 cm²	0.9965	7.2637	44.3312	3.2089
0.05 cm²	0.9943	9.0254	43.7668	3.9276		1.00	7.46	44.82	3.34
0.05 cm²	0.9961	9.0246	43.9616	3.9519	Device Size	Voc (V)	Jsc (mAcm-2)	FF (%)	PCE (%)
	1.00	8.86	44.26	3.92	0.36 cm²	1.0044	7.2511	45.8913	3.3423
Device Size	Voc (V)	Jsc (mAcm-2)	FF (%)	PCE (%)	0.36 cm²	1.0019	7.1621	45.5944	3.2718
0.09 cm²	0.9892	8.8941	44.1323	3.8829		1.00	7.21	45.74	3.31
0.09 cm²	0.9926	9.2197	43.3003	3.9625	0.36 cm²				
0.09 cm²	0.9916	9.2109	42.6365	3.8943					
	0.99	9.11	43.36	3.91					

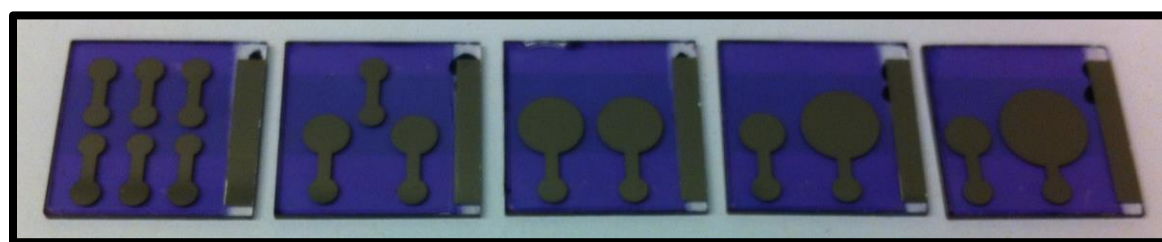


Table S9. Device statistics for **PDTT-BOBT:PDI-DPP-PDI** devices in final optimized screening.

Processing	Voc (V)	Jsc (mAcm-2)	FF (%)	PCE (%)
As-cast	1.0294	5.3697	34.8453	1.9261
As-cast	1.0258	4.8641	34.1100	1.7019
As-cast	1.0229	4.8362	34.2848	1.6960
As-cast	1.0276	5.4073	34.4377	1.9136
	1.03	5.12	34.42	1.81
Processing	Voc (V)	Jsc (mAcm-2)	FF (%)	PCE (%)
SVA 4 min	0.9906	9.8910	45.6477	4.4728
SVA 4 min	0.9880	9.1990	45.4850	4.1341
SVA 4 min	0.9901	9.5116	43.5553	4.1018
SVA 4 min	0.9980	9.9120	44.5890	4.4110
	0.99	9.63	44.82	4.28

Control Devices

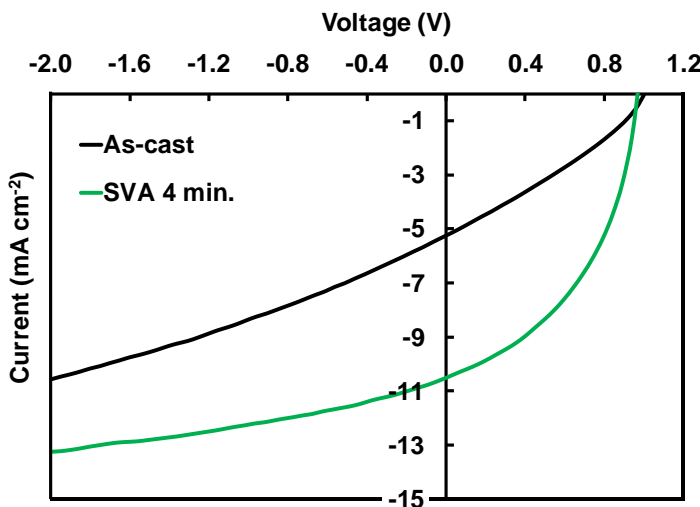


Figure S24. Current voltage curves for **PTB7-Th:PDI-DPP-PDI** control devices.

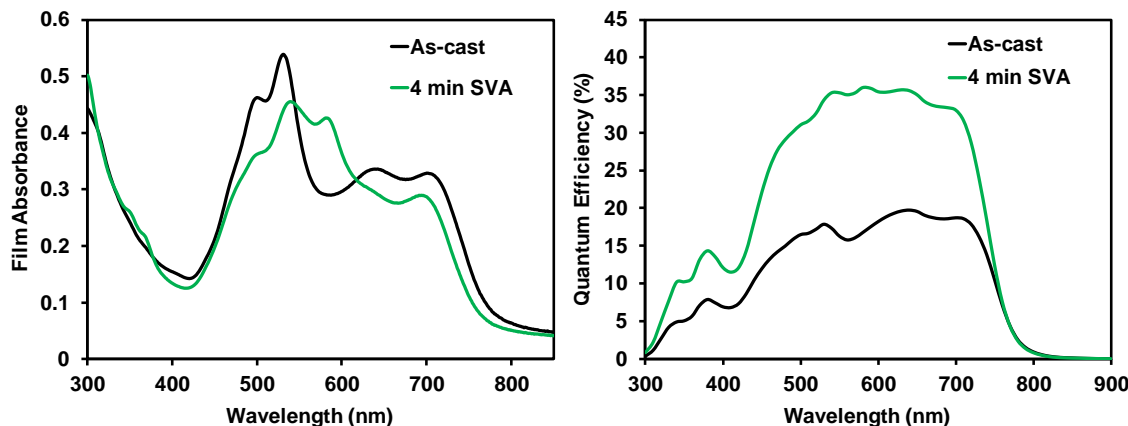


Figure S25. Optical absorption profiles (left) external quantum efficiencies (right) for **PTB7-Th:PDI-DPP-PDI**.

Table S10. Device statistics for **PTB7-Th:PDI-DPP-PDI** control devices.

PTB7-Th:PDI-DPP-PDI As-cast	Voc (V)	Jsc (mAcm-2)	FF (%)	PCE (%)
	1.007294	5.238871	30.21127	1.594274
	1.008543	5.349355	29.74575	1.604799
	1.000214	5.274644	30.84561	1.627344
1.005955	5.293142	31.16262	1.659305	
	1.01	5.29	30.5	1.6
Best in Literature	0.97	6.41	35.20	2.2
PTB7-Th:PDI-DPP-PDI SVA	Voc (V)	Jsc (mAcm-2)	FF (%)	PCE (%)
	0.9617	11.2572	42.1452	4.5627
	0.9688	10.9286	43.5634	4.6123
	0.9664	10.5498	45.1400	4.6023
0.9641	10.6259	45.1454	4.6250	
	0.97	10.84	44.0	4.6
Best in Literature	0.98	11.32	50.1	5.6

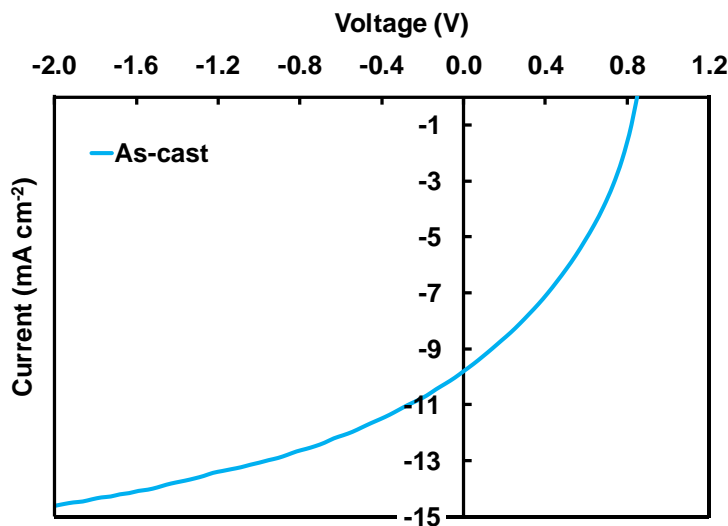


Figure S26. Current voltage curves for PDTT-BOBT:PC₆₁BM control devices.

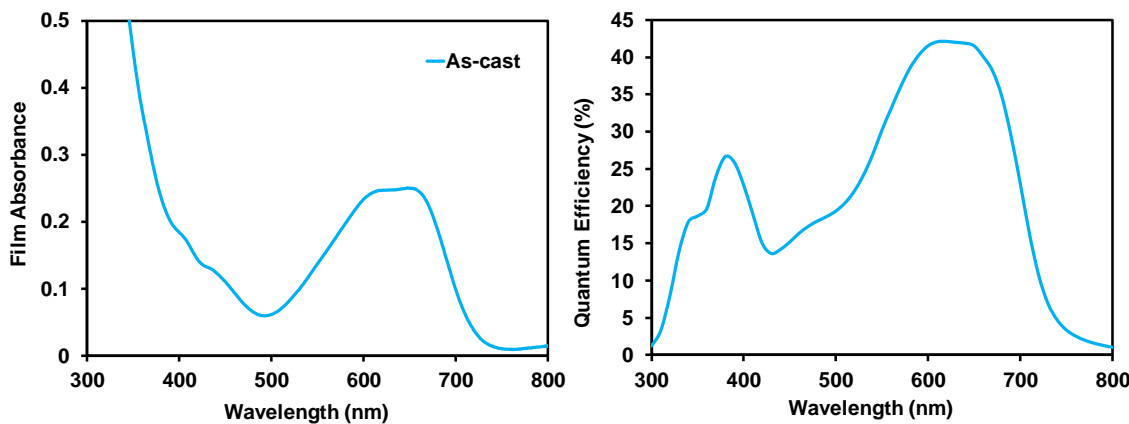


Figure S27. Optical absorption profiles (left) external quantum efficiencies (right) for PDTT-BOBT:PC₆₁BM.

Table S11. Device statistics for PDTT-BOBT:PC₆₁BM control devices.

PDTT-BOBT:PC ₆₁ BM As-cast	Voc (V)	Jsc (mAcm ⁻²)	FF (%)	PCE (%)
	0.8494	9.2726	37.4002	2.9458
	0.8463	9.4320	37.0278	2.9556
	0.8404	9.5277	36.8803	2.9529
	0.8532	9.4453	37.0747	2.9878
	0.8466	9.7969	37.4304	3.1046
	0.8506	9.6171	37.5970	3.0757
	0.85	9.52	37.24	3.00

Device Stability

Thermal Stability – The thermal stability of **PDTT-BOBT:PDI-DPP-PDI** was measured by heating a device at 80 °C in air for 60 minutes. At 10, 20, 40 and 60 minute intervals the device performance was measured once the device had reached room temperature. The EQE profiles were obtained from the initial device and at the end of the thermal experiments.

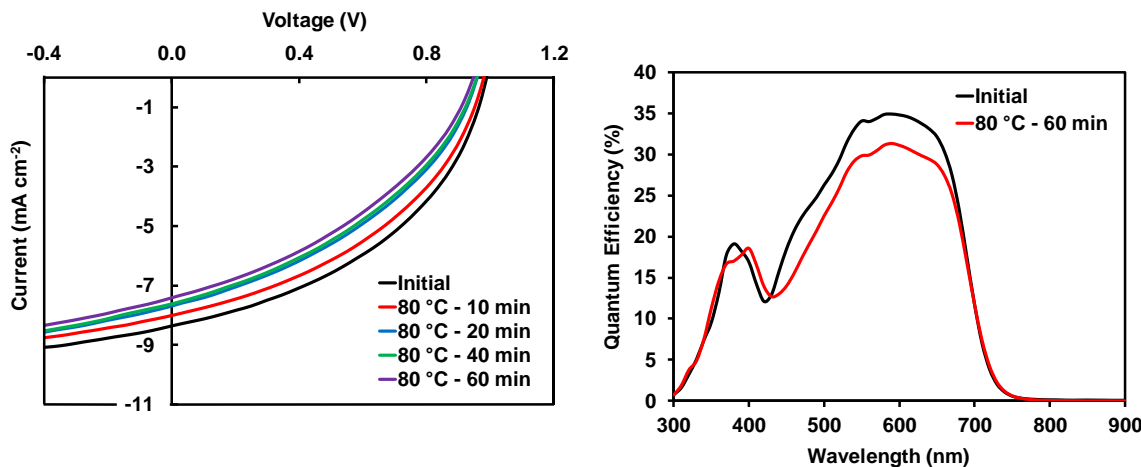


Figure S28. Current voltage curves for **PDTT-BOBT:PC₆₁BM** control devices (left) and EQE profiles (right).

Table S12. Device statistics for **PDTT-BOBT:PC₆₁BM** thermal stability measurements.

Time at 80 °C	Voc (V)	Jsc (mAcm-2)	FF (%)	PCE (%)
0	0.99	8.89	43.92	3.85
10	0.98	8.52	42.31	3.53
20	0.96	8.14	40.07	3.13
40	0.96	8.03	39.57	3.04
60	0.95	7.85	38.85	2.88

Air/Light Stability – The air and light stability of **PDTT-BOBT:PDI-DPP-PDI** was measured from three different devices. One device was left in air with no light exposure, a second was left in air under ambient light and a third was left in air in direct sunlight. Device performance, absorption profiles and EQE profiles were measured 14 days after exposure to these various conditions.

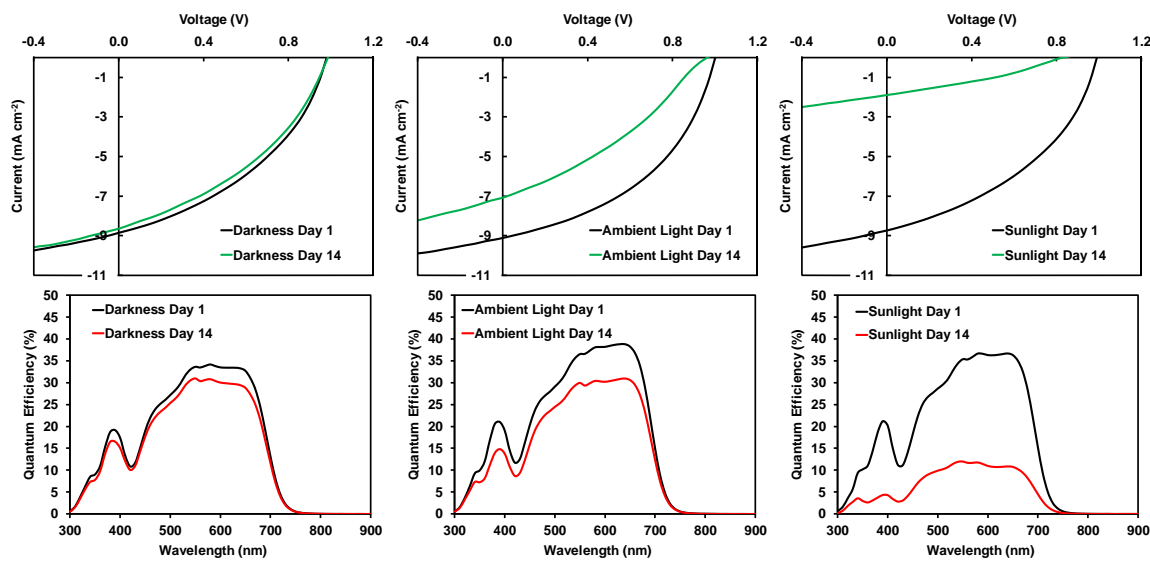


Figure S29. Current voltage curves for **PDTT-BOBT:PDI-DPP-PDI** air/light stability devices (top) and their respective external quantum efficiencies (bottom).

Table S13. Device results for **PDTT-BOBT:PDTT-BOBT** air/light stability measurements.

Sunlight	Voc (V)	Jsc (mA cm^{-2})	FF (%)	PCE (%)
Day 1	0.99	9.35	41.54	3.85
Day 14	0.84	2.02	32.05	0.54
Ambient Light	Voc (V)	Jsc (mA cm^{-2})	FF (%)	PCE (%)
Day 1	1.00	9.66	44.64	4.31
Day 14	0.96	7.49	33.30	2.41
Darkness	Voc (V)	Jsc (mA cm^{-2})	FF (%)	PCE (%)
Day 1	0.98	9.46	40.89	3.79
Day 14	0.99	9.27	38.74	3.54

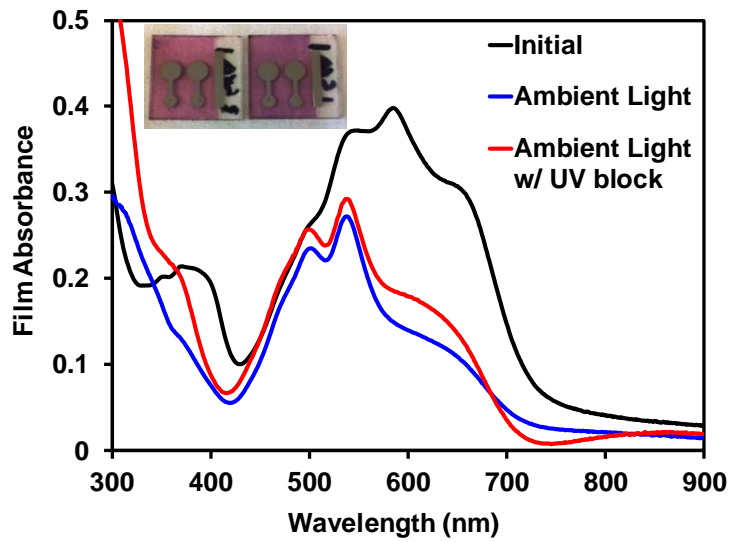


Figure S30. Optical absorption profiles of **PDTT-BOBT:PDI-DPP-PDI** under air/light stability conditions with and without UV-light protection.

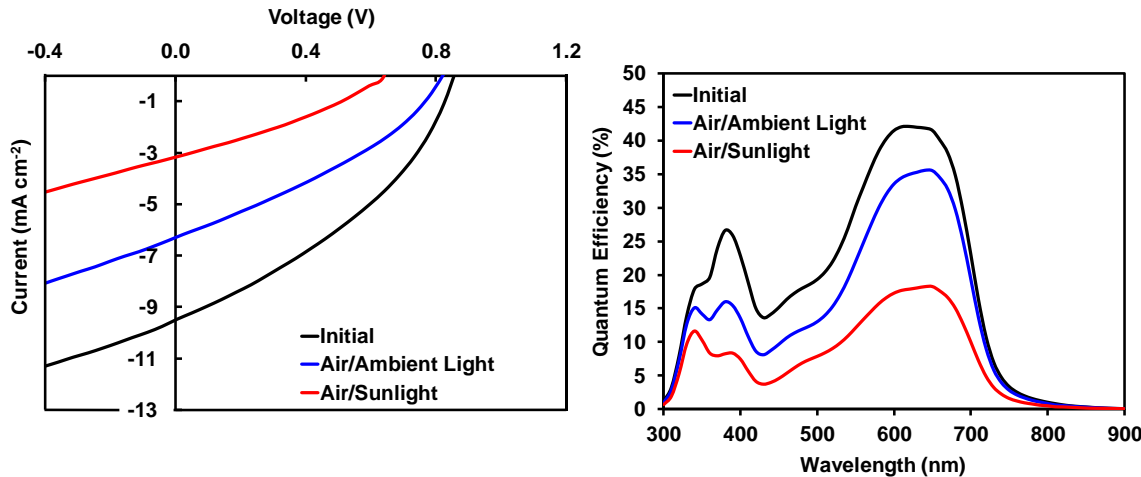


Figure S30. Current voltage curves for **PDTT-BOBT:PC₆₁BM** air/light stability devices (left) and their respective external quantum efficiencies (right).

Table S13. Device results for **PDTT-BOBT:PC₆₁BM** air/light stability measurements.

	Voc (V)	Jsc (mAcm ⁻²)	FF (%)	PCE (%)
Initial	0.86	9.51	37.17	3.03
Ambient Light	0.82	6.30	33.90	1.75
Sunlight	0.65	3.17	31.59	0.65

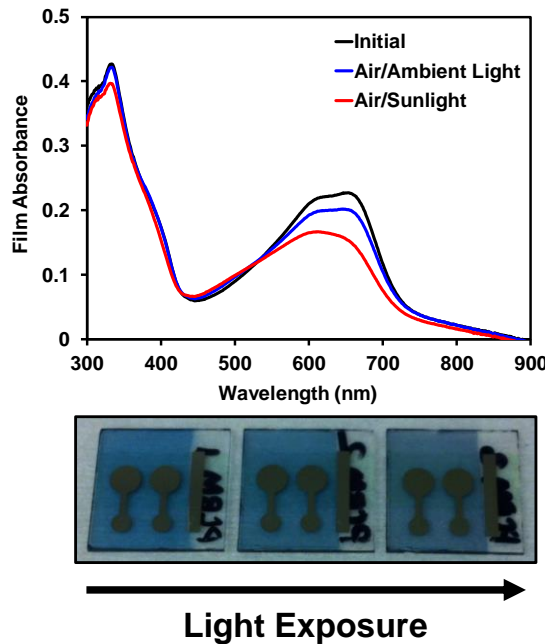


Figure S32. Optical absorption profiles of **PDTT-BOBT:PC₆₁BM** under air/light stability conditions.

Active layer thickness

The active layer thickness was measured by atomic force microscopy. A thin-film of **PDTT-BOBT:PDI-DPP-PDI** cast on an ITO/glass substrate was cut down to the substrate with a scalpel and it scanned at 50X50 mm, then the thickness of the film was measured by measuring the profile left from the scalpel using Gwyddion software program.

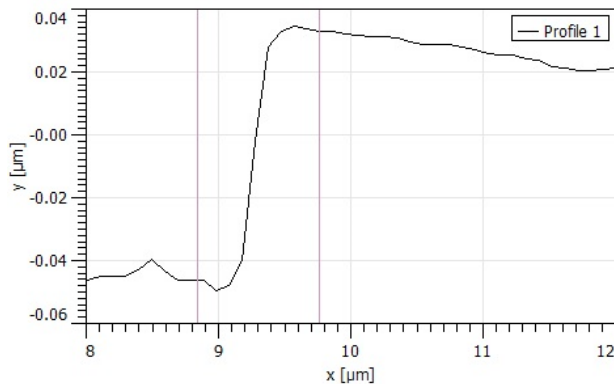


Figure S33. Plot measuring the active layer thickness of **PDTT-BOBT:PDI-DPP-PDI** cast with optimized processing conditions onto an ITO/glass substrate.

The active layer thickness was measured by atomic force microscopy. A thin-film of **PDTT-BOBT:PDI-DPP-PDI** cast on an ITO/glass substrate was cut down to the substrate with a scalpel and it scanned at 50X50 mm, then the thickness of the film was measured by measuring the profile left from the scalpel using Gwyddion software program.

Solution UV-vis spectra

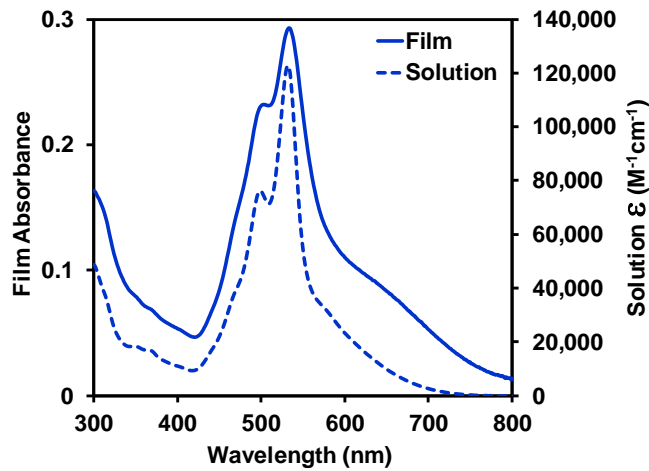


Figure S34. Solution and thin-film optical absorption profiles of **PDI-DPP-PDI**. Full characterization data can also be found in our previous work.^{2,5}

References

- 1J. Pommerehne, H. Vestweber, W. Guss, R. F. Mahrt, H. Bässler, M. Porsch and J. Daub, *Adv. Mater.*, 1995, **7**, 551–554.
- 2S. M. McAfee, S. V. Dayneko, P. Josse, P. Blanchard, C. Cabanetos and G. C. Welch, *Chem. Mater.*, 2017, **29**, 1309–1314.
- 3G. P. Kini, S. K. Lee, W. S. Shin, S.-J. Moon, C. E. Song and J.-C. Lee, *J. Mater. Chem. A*, 2016, **4**, 18585–18597.
- 4Y. Sun, J. H. Seo, C. J. Takacs, J. Seifter and A. J. Heeger, *Adv. Mater.*, 2011, **23**, 1679–1683.
- 5S. M. McAfee, S. V. Dayneko, A. D. Hendsbee, P. Josse, P. Blanchard, C. Cabanetos and G. C. Welch, *J. Mater. Chem. A*, 2017, **5**, 11623–11633.